

# Fast Pose Verification for High-Speed Radiation Therapy

Andreas Maier<sup>1,2</sup>, Susanne Westphal<sup>1</sup>, Tobias Geimer<sup>1,2</sup>, Peter G. Maxim<sup>3</sup>,  
Gregory King<sup>3</sup>, Emil Schueler<sup>3</sup>, Rebecca Fahrig<sup>4</sup>, Billy Loo<sup>3</sup>

<sup>1</sup>Friedrich-Alexander Universität Erlangen-Nürnberg

<sup>2</sup>Graduate School in Advanced Optical Technologies (SAOT)

<sup>3</sup>Radiation Oncology, Stanford University Medical Center

<sup>4</sup>Radiological Sciences Lab, Stanford University

e-mail

**Abstract.** This paper discusses fast pose verification for radiation therapy on a new high-speed radiation therapy device. The PHASER system follows the idea of 4<sup>th</sup> generation CT imaging and allows fast 360° treatment using a steerable electron beam. Doing so, dose delivery is possible in few seconds. A major problem, however, is fast verification of the patient pose during treatment. In this paper, we suggest to use a projection-based approach that can be evaluated quickly and allows an accuracy below 1 mm as shown by our simulation study based on planning data from six 4-D CT data sets.

## 1 Introduction

Patient motion is a major problem for imaging [1] and radiation therapy [2]. In radiation therapy, dose delivery is typically planned on a 3-D CT image [3] and high attention is paid to align the patient's actual position at the treatment site with the planning scan [4]. For tumors in the head and neck region, this can be achieved by the use of an immobilization mask [5] which prevents head motion by fixating the patient to the couch. Due to the long duration of the radiation treatment, there is also motion that cannot be avoided completely. In particular, respiratory motion may cause the target area to move up to 2 *cm* [6]. Without compensation, this would cause the dose to be delivered to the wrong location, resulting in damaged healthy tissues and more importantly the potential survival of the malignant tumor itself [7]. In order to compensate for this, many approaches have been suggested ranging from implanted gold markers [8] to the use of respiratory surrogate signals [9,10] and the prediction of dense deformation fields [11,12]. In summary, these methods are feasible, but come at significant additional efforts.

In this work, we focus on a different treatment device that has been suggested by Maxim and Loo [13]. The Pluridirectional High-Energy Agile Scanning Electron Radiotherapy (PHASER) System is able to deliver the entire treatment dose within only a few seconds and, therefore, provides a treatment duration range

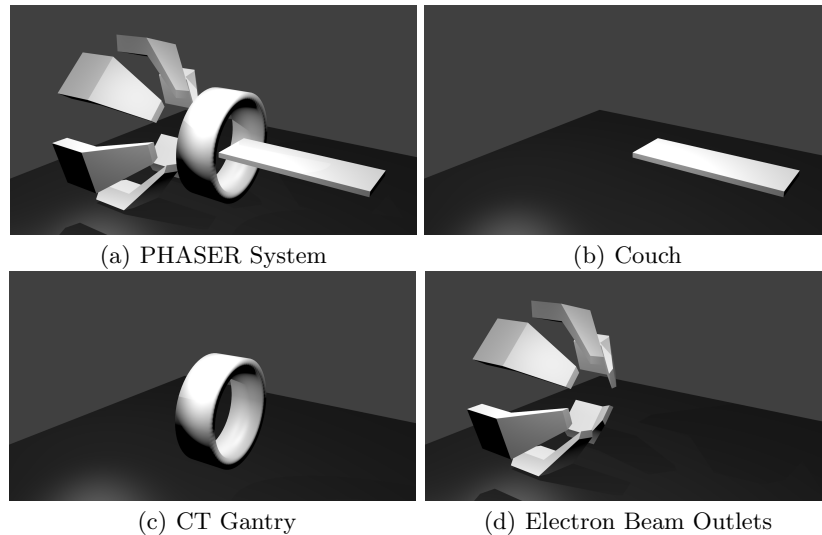


**Fig. 1.** A schematic of the PHASER system (a) with its main parts: The couch (b), the CT Gantry (c), and the electron beam outlets (d)

that can effectively compensate for respiratory motion by a simple breath hold command. Additionally, in contrast to traditional radiation therapy, electrons instead of photons are used to deliver the radiation dose. This way, energy can be deposited much faster using fewer particles and with higher accuracy [14]. Fig. 1 shows a schematic of the system.

## 2 Materials and Methods

### 2.1 PHASER System

While delivering such high amounts of dose in such short time has many advantages, it also poses special challenges to the imaging. In order to image the patient quickly, a special CT gantry was designed [15]. The associated detector is curved on a circle segment with a diameter of 1300 mm, an arc length of 1024 mm and a detector height of 192 mm. The detector provides high resolution in the center of the field-of-view (FOV) while offering larger pixels towards the outside of the FOV which typically is of lower interest for the purpose of radiation therapy. Fig. 2 shows the FOV for two typical imaging locations.

### 2.2 Pose Verification

In contrast to typical radiation therapy, the PHASER system allows only very little time to verify the patient pose and deliver the dose. The whole process must be completed within a single breath-hold. As patients often suffer from

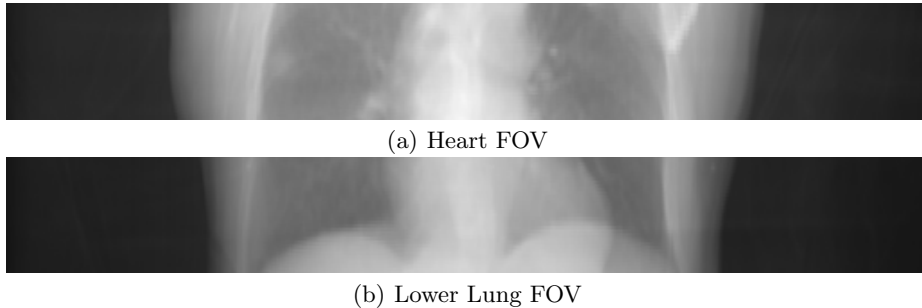


**Fig. 2.** The CT detector that was developed for the PHASER system offers a slightly larger field-of-view than a traditional CT detector.

impaired lung function, we assume this period to be within the range of 12 to 16 seconds [16]. Therefore, computationally expensive approaches that require reconstruction and motion compensation are not applicable [6]. Furthermore, we do not want to create an additional burden to the patients by using e.g. implanted gold markers [5].

The current work-flow on the PHASER system will involve a high-quality CT scan, registration to the planning CT, and an adaptation of the treatment plan [15] to accommodate the current patient position. Hence, we expect the motion during the treatment to emerge only from respiratory motion.

In order to compensate for the current motion state, we propose to use projection-based imaging only, based on projections of the 4-D planning CT. In addition, we reuse a lung segmentation that is created during the planing procedure for the pose verification process. In the following, we denote the projection of the mask as  $\mathbf{m}_{i,\theta} \in \mathbb{R}^N$  for the  $i^{\text{th}}$  motion state and projection angle  $\theta$  where  $N$  is the number of pixels. The projection of the planning in state  $i$  is denoted as  $\mathbf{p}_{i,\theta} \in \mathbb{R}^N$  while the current projection is  $\mathbf{p}_\theta \in \mathbb{R}^N$ . This allows us to identify the two motion states  $i_1^*$  and  $i_2^*$  that are closest to  $\mathbf{p}_\theta$  using

$$i^* = \operatorname{argmin}_i f(\mathbf{p}, i) = \sum_{\theta} \|\mathbf{m}_{i,\theta} \cdot (\mathbf{p}_{i,\theta} - \mathbf{p}_\theta)\|_1 \quad (1)$$

where  $\cdot$  denotes the element-wise vector product. For the experimental evaluation, we chose to sample  $\theta$  at 18 equiangular positions over  $360^\circ$  of gantry rotation. The estimated tumor position  $\hat{\mathbf{t}} \in \mathbb{R}^3$  can now be estimated as the weighted mean position between  $\mathbf{t}_{i_1^*}$  and  $\mathbf{t}_{i_2^*}$ .

### 2.3 Patient Data

Patient data from six patients that underwent regular lung tumor radiation therapy were used to investigate the accuracy of the proposed approach. For each patient, there were two 4-D CT scans with 10 motion states in each available, one scan from the beginning of the treatment and one four weeks later, after

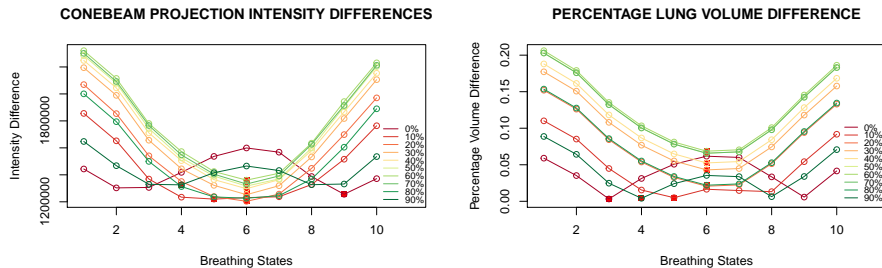


**Fig. 3.** The proposed measure (left) exhibits a high correlation with the relative volumetric change between two breathing states (right).

the therapy was finished. The volumes were sampled at a voxel size of  $0.98 \times 0.98 \times 2.0 \text{ mm}^3$ . After tumor segmentation, the average tumor centroid motion in these patients was determined at  $2.50 \pm 2.10 \text{ mm}$ . This low amount of motion is related to the fact that the tumors were mainly localized in the top of the lung and that patients with lung cancer typically also exhibit functional losses associated with low changes in lung volume (cf. Fig. 3).

### 3 Results

Fig. 3 shows the behavior of the measure proposed in Eq. 1 compared to the relative change in lung volume for Patient 1. It can be observed that states with a similar lung volume also show similar values in  $f(\mathbf{p}, i)$ . We observed a similar relation in the other five patients.

In a second experiment, we excluded one of the breathing phases from the data and performed a leave-one-out evaluation to estimate the accuracy of unknown breathing motion. Table 1 presents these localization accuracies. We observe that the average error is much below the maximal tumor motion. This results in an average error of  $0.80 \pm 0.25 \text{ mm}$  compared to  $2.50 \pm 2.10 \text{ mm}$  maximal tumor motion. In the case with the largest tumor motion of 7 mm the error is reduced down to 0.83 mm.

### 4 Discussion

From the experimental results, we observed that the localization accuracy is on average below 1 mm. Compared to current clinical safety margins of about 7 mm even for motion compensated treatment, this is a great reduction. However, one has to be careful with the interpretation of the results, as the average motion in our patients was only  $2.50 \pm 2.10 \text{ mm}$ . Thus, our error is well below the maximal motion, but also higher than one would expect given that the motion was sampled ten times. This is related to the resolution of our 4-D CT scan that had a

Patient ID	Acquisition Date	RMSE [mm]	$t_{\max}$ [mm]
Patient 1	2015-10	$0.64 \pm 0.31$	2.0
Patient 1	2015-11	$0.62 \pm 0.30$	2.0
Patient 2	2015-11	$1.01 \pm 0.71$	7.0
Patient 2	2015-12	$0.82 \pm 0.48$	7.0
Patient 3	2013-11	$0.98 \pm 0.62$	1.5
Patient 3	2013-12	$0.72 \pm 0.56$	1.5
Patient 4	2014-12	$1.18 \pm 0.75$	2.0
Patient 4	2015-01	$1.12 \pm 0.78$	2.0
Patient 5	2014-06	$0.36 \pm 0.22$	0.5
Patient 5	2014-07	$0.40 \pm 0.18$	0.5
Patient 6	2014-04	$0.83 \pm 0.59$	2.0
Patient 6	2014-05	$0.80 \pm 0.58$	2.0
<b>Average</b>		<b><math>0.80 \pm 0.25</math></b>	<b><math>2.50 \pm 2.10</math></b>

**Table 1.** Overview on the localization accuracy using leave-one-motion-state-out-evaluation.

voxel size of  $0.98 \times 0.98 \times 2.0 \text{ mm}^3$ . In case of our patients, the main magnitude of motion occurs along the  $z$  axis, i.e. our results lie below the accuracy of one voxel. In future studies, we will have to verify whether this low amount of motion occurs in more patients with lung cancer. As a result, we would have to increase the resolution of the planning CT in the affected directions to alleviate the problem. A possible solution for this problem would be adaptive detector binning [17]. Nonetheless even with the current setup, patients with large tumor motion benefit greatly from the method. In the patient with the large tumor motion of 7 mm, the error could be reduced down to 0.8 mm thereby preventing incorrect deposition of the radiation dose.

Another challenge that we plan to investigate in future work is continuous treatment using precomputed 4-D treatment plans for patients such as young children who cannot follow breathing commands. With the current system setup, we would be able to select the correct treatment plan for the current motion state in real-time.

## References

1. Nehmeh SA, Erdi YE. Respiratory Motion in Positron Emission Tomography/Computed Tomography: A Review. *Seminars in Nuclear Medicine: Developments in Instrumentation*. 2008;38(3):167 – 176.
2. Korreman SS. Motion in radiotherapy: photon therapy. *Physics in Medicine and Biology*. 2012;57(23):R161.
3. Censor Y, Altschuler MD, Powlis WD. A computational solution of the inverse problem in radiation-therapy treatment planning. *Applied Mathematics and Computation*. 1988;25(1):57 – 87.

4. Bauer S, Wasza J, Haase S, Marosi N, Hornegger J. Multi-modal Surface Registration for Markerless Initial Patient Setup in Radiation Therapy using Microsoft's Kinect Sensor. In: IEEE International Conference on Computer Vision (ICCV) Workshops; 2011. p. 1175–1181.
5. Chen S, Lu Y, Hopfgartner C, Sühling M, Steidl S, Hornegger J, et al. 3-D Printing Based Production of Head and Neck Masks for Radiation Therapy Using Ct Volume Data: A Fully Automatic Framework. In: IEEE International Symposium on Biomedical Imaging: From Nano to Macro. Prague, Czech Republic; 2016. p. 403–406.
6. Bögel M, Hofmann HG, Hornegger J, Fahrig R, Britzen S, Maier A. Respiratory motion compensation using diaphragm tracking for cone-beam c-arm CT: a simulation and a phantom study. *Journal of Biomedical Imaging*. 2013;2013:6.
7. Shepard DM, Ferris MC, Olivera GH, Mackie TR. Optimizing the Delivery of Radiation Therapy to Cancer Patients. *SIAM Review*. 1999;41(4):721–744.
8. Huang CY, Tehrani JN, Ng JA, Booth J, Keall P. Six degrees-of-freedom prostate and lung tumor motion measurements using kilovoltage intrafraction monitoring. *International Journal of Radiation Oncology\* Biology\* Physics*. 2015;91(2):368–375.
9. Bögel M, Maier A, Hofmann HG, Hornegger J, Fahrig R. Diaphragm tracking in cardiac C-Arm projection data. In: *Bildverarbeitung für die Medizin 2012*. Springer Berlin Heidelberg; 2012. p. 33–38.
10. Wasza J, Fischer P, Leutheuser H, Oefner T, Bert C, Maier A, et al. Real-Time Respiratory Motion Analysis Using 4-D Shape Priors. *IEEE Transactions on Biomedical Engineering*. 2016;63(3):485–495.
11. Taubmann O, Wasza J, Forman C, Fischer P, Wetzl J, Maier A, et al. Prediction of Respiration-Induced Internal 3-D Deformation Fields From Dense External 3-D Surface Motion. In: *Computer Assisted Radiology and Surgery (CARS), 28th International Congress and Exhibition*. International Journal of Computer Assisted Radiology and Surgery. Heidelberg; 2014. p. 33–34.
12. Geimer T, Unberath M, Taubmann O, Bert C, Maier A. Combination of Markerless Surrogates for Motion Estimation in Radiation Therapy. In: *Computer Assisted Radiology and Surgery (CARS), 30th International Congress and Exhibition*; 2016. p. 59–60.
13. Maxim PG, Loo BW. Pluridirectional High-Energy Agile Scanning Electron Radiotherapy (PHASER): Extremely Rapid Treatment for Early Lung Cancer. *DTIC Document*; 2015.
14. Bazalova-Carter M, Qu B, Palma B, Hårdemark B, Hynning E, Jensen C, et al. Treatment planning for radiotherapy with very high-energy electron beams and comparison of VHEE and VMAT plans. *Medical Physics*. 2015;42(5):2615–2625.
15. Kemmerling EMC, Wu M, Yang H, Maxim PG, Loo Jr BW, Fahrig R. Optimization of an on-board imaging system for extremely rapid radiation therapy. *Medical Physics*. 2015;42(11):6757–6767.
16. Rosenzweig KE, Hanley J, Mah D, Mageras G, Hunt M, Toner S, et al. The deep inspiration breath-hold technique in the treatment of inoperable non-small-cell lung cancer. *International Journal of Radiation Oncology\* Biology\* Physics*. 2000;48(1):81–87.
17. Steg A, Reichenbach M, Söll C, Shi L, Maier A, Riess C. Dynamic Pixel Binning allows Spatial and Angular Resolution Tradeoffs to Improve Image Quality in X-Ray C-Arm CT. In: *International Symposium on Biomedical Imaging*; 2016. .